Design and Analysis of Turbulence Grids for Aeroacoustic Measurements

Luke Bowen*, Alper Celik†, Mahdi Azarpeyvand‡
Faculty of Engineering, University of Bristol, BS8 1TR, UK

Carlos R. Ilário da Silva§
Embraer, Sáo José dos Campos, 12227-901, Brazil

The effect of turbulence generating passive grids and their self noise has been studied. The geometric properties of the grids and the position within the tunnel contraction nozzle were varied to influence of turbulence generation. The resulting flow conditions and far field noise emission was analysed. A total of 12 passive grids were tested, all with square shaped bars of various bar diameter and mesh sizes, where each grids' flow properties were characterised and the far field noise was measured. It was found that grids closer to the contraction nozzle exit showed higher levels of turbulence intensity with the penalty of a sound spectra contaminated with the grids' self noise. Grids further upstream of the contraction nozzle exit offered lower self noise but the spectra was still contaminated with tones and broadband humps. However, the grids positioned furthest upstream from the contraction nozzle exit showed that it could generate similar levels of turbulence intensity to grids closest to the contraction nozzle exit without the self noise of the grid affecting the normal running background noise of the wind tunnel. In a case study using a NACA 0012 airfoil it was found that the interaction noise was sensitive to the geometry of the grids.

I. Nomenclature

a_N	=	Contraction nozzle height [mm]
a_G	=	Grid height [mm]
b_N	=	Contraction nozzle width [mm]
b_G	=	Grid width [mm]
C	=	Contraction ratio [-]
d	=	Bar diameter [mm]
f	=	Frequency [Hz]
k_e	=	Wavenumber range of energy-containing eddies [-]
k_x	=	Streamwise wavenumber [-]
M	=	Mesh size [mm]
p	=	Pressure [Pa]
p'	=	Pressure fluctuation [Pa]
p_{ref}	=	Reference pressure $2x10^{-5}$ [Pa]
PSD	=	Power spectral density [dB/Hz]
U_∞	=	Free-stream velocity [m/s]
u	=	Streamwise velocity fluctuation [m/s]
x_G	=	Streamwise distance between contraction nozzle and grid location [mm]
Γ	=	Gamma function [-]
Λ	=	Integral Length Scale [mm]
σ	=	Solidity ratio [-]
ϕ_{pp}	=	Power spectral density of the pressure fluctuation [dB/Hz]

*Ph.D Student, Department of Mechanical Engineering, luke.bowen@bristol.ac.uk
†Postdoctoral Research Associate, Department of Mechanical Engineering, alper.celik@bristol.ac.uk
‡Professor of Aerodynamics and Aeroacoustics, Department of Mechanical Engineering, m.azarpeyvand@bristol.ac.uk
§Challenge Owner in Electrifying Aviation, Embraer, Sáo José dos Campos, Brazil, carlos.ilario@embraer.com.br

ϕ_{uu} = Power spectral density of the streamwise velocity fluctuation [dB/Hz]
ω = Angular frequency [rad/s]

II. Introduction

Turbulence interaction noise is an important noise generation mechanism, and with the recent influx in studies on passive leading edge treatments, be that serrations [1–4] or porous materials [5–7] to name a few, turbulence generation for aeroacoustic facilities is an important consideration. Generally, passive grid generated turbulence is a highly studied field and there is a lot of information regarding the design of grids for aerodynamic measurements [8–13]. A passive grid with simple homogeneous geometric properties will tend to produce homogeneous, nearly isotropic turbulence from 10 mesh lengths downstream [9]. To further improve the isotropy, it is generally considered that a contraction ratio of 1.3 is preferable, to strain the turbulence and to equal the isotropy between the three components of velocity fluctuation [12]. For open-jet aeroacoustic facilities, however, this becomes a more complex problem. The two main types of study that have been researched are facilities with high contraction ratios utilising grids far inside contraction nozzle, and facilities that attach grids to the nozzle outlet. Chaitanya *et al*. [14] used the first arrangement at Southampton University to identify airfoil geometry effects on turbulence interaction noise, and direct far field noise measurement was possible due to the grid being far inside the contraction nozzle. Geyer *et al.* [7] produced a study on leading edge noise that used multiple grids at the contraction nozzle outlet of the facility at Brandenburg University of Technology. To measure the far field noise the beamforming microphone array technique was used and highlighted a small study between three grids, but concluded that turbulence generation deserved further study [7]. This study aims to identify conditions for generating appropriate levels of turbulence, without compromising the ability to carry out direct measurement of the radiated far field noise due to contamination from the self noise produced by the grid.

The aim of the study is to present the far field noise generated by turbulence grids in an aeroacoustic facility. It examines the changes in geometry and grid size and how that affects the turbulence generated at the nozzle exit and the far field noise. The process for the design of turbulence grids for aerodynamic measurements is a well documented process in literature and passive grid design is shown to be an effect method for studies in isotropic turbulence. As most aeroacoustic facilities consist of a large contraction that opens into an anechoic chamber, there is scope for a study that assesses the design of turbulence grids for these facilities. The main parameter that needs to be considered is the self noise that the grid generates in order not to hinder the facilities' ability to carry out direct noise measurement of turbulence interaction noise. The contraction ratio between the location of the grid and the outlet of the nozzle is an important consideration. A grid that is subject to the free-stream velocity at the nozzle outlet will dominate the noise spectra and noise from an airfoil will be lost amongst the grid self-noise, although it will generate strong turbulent characteristics. As the grid moves further into the contraction its effectiveness of generating turbulence could be hindered due to the reduced impingement velocity, and straining of the structures within the large contraction may affect the isotropy of the generated turbulence. However, the reduction of the impingement velocity will reduce the level of self-noise that the grid will generate. Therefore, this study explores the effect of the grids position within the contraction nozzle, as well as its geometric properties at each of these locations.

III. Measurement setup

The experiments were performed in the University of Bristol Aeroacoustic Facility, which is a closed-circuit, open-jet anechoic wind tunnel. This is shown in Fig. 1, with a turbulence grid within the contraction nozzle and a hot-wire probe mounted in the flow. The chamber is anechoic down to 160Hz with physical dimensions of 6.7 m x 4.0 m x 3.3 m and the nozzle has the dimensions of 500 mm x 775 mm which allows a steady operation from 5 m/s to 45 m/s and a normal turbulence intensity level below 0.2% [15]. Far field noise measurements were made using 23 1/4 inch GRAS 40PL microphones which have a large dynamic range and an upper limit of 142 dB, covering a frequency range between 10 Hz and 20,000 Hz. 23 of these microphones were arranged on to a far field array arc allowing measurement between 35° and 150° polar angles at a distance of 1.75m from the center of the jet core.

The turbulent flow was characterised using Constant Temperature Anemonetry Hot-wire. A Dantec 55P16 single hot-wire probe was used to measure the stream-wise component of velocity, which was operated using a Dantec Streamline Pro system with CTA91C10 module and the probe was calibrated daily using a Dantec 54H10 calibrator. The measurements were sampled at a rate of 2^{15} Hz for 32 seconds using a National Instruments PXIe-4499 module mounted in a National Instruments PXIe-1026Q chassis.

To generate the oncoming turbulence, a set of grids were designed to be positioned upstream of the nozzle exit.

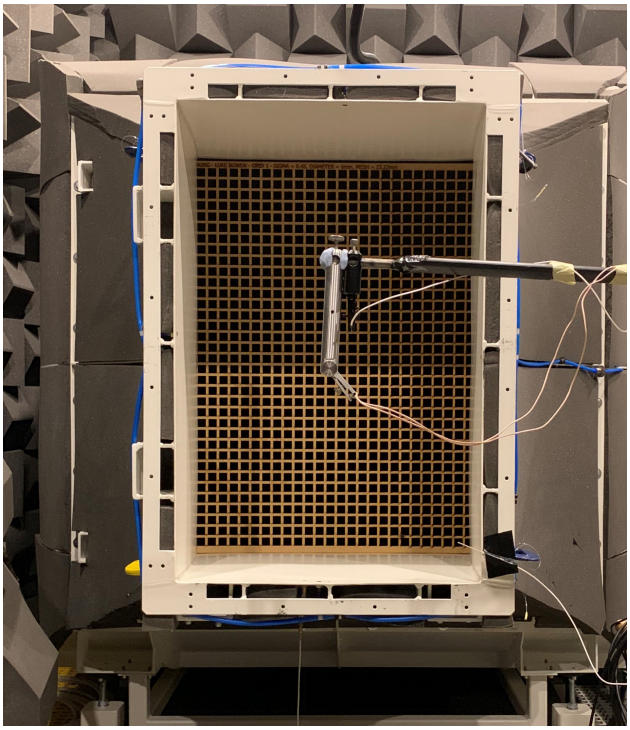

Fig. 1 A small turbulence grid within the wind tunnel contraction nozzle.

Table 1 The geometric properties of the nozzle and each turbulence grid,.

Grid Location	Height, a (mm)	Width, b (mm)	x_G (mm)	C
A	838	613	500	1.3
B	1023	911	820	2.4
C	1305	1305	1040	4.4

Figure 2 displays a schematic of the contraction nozzle with the three grid positions denoted by x_G, the contraction nozzle outlet size is defined by a_N and b_N, the grid size is defined by a_G and b_G. From the geometry definitions in the figure the contraction ratio is considered as, $C = (a_G \cdot b_G)/(a_N \cdot b_N)$, which is the ratio of the area of the grid, to the area of the nozzle outlet. For aerodynamic purposes, a mesh grid can be used within a contraction to produce isotropic homogeneous turbulence. This is a widely documented procedure in aerodynamics and the use of grids has been well researched, ideally a contraction ratio of 1.3 is desired for the production of isotropic turbulence [12]. For the case of turbulence generation for aeroacoustic facilities, there must be more consideration taken into the grid design. Changes in the grid geometry can affect the generation and initial conditions of the turbulence, which in turn affects the downstream properties of fully developed turbulence [10, 11]. Varying geometric properties on the grids and its affect on the generated noise is an area that lacks insight and the purpose of this study is to document these effects. The geometry that was varied was the mesh size (m), bar diameter (d) and solidity factor (σ) which is the measure of cross-sectional area of the grid to the total area of the grid. These parameters are demonstrated by Fig. 3a and σ is calculated from,

$$\sigma = d/M(2 - d/M). \tag{1}$$

The ratio between the cross-sectional area at the point where the grid was mounted and the nozzle exit, c, was also studied. This included 3 different locations for the grids within the contraction nozzle, as displayed in Fig. 2. Table 2 gives the geometric parameters for the 12 grids that were tested in this study. Square bar grids were used as these are known to be quieter, and generate higher levels of turbulence than round bars [16]. The grids were manufactured by cutting square perforations in to Medium-density fibreboard (MDF) which generated the desired mesh size and

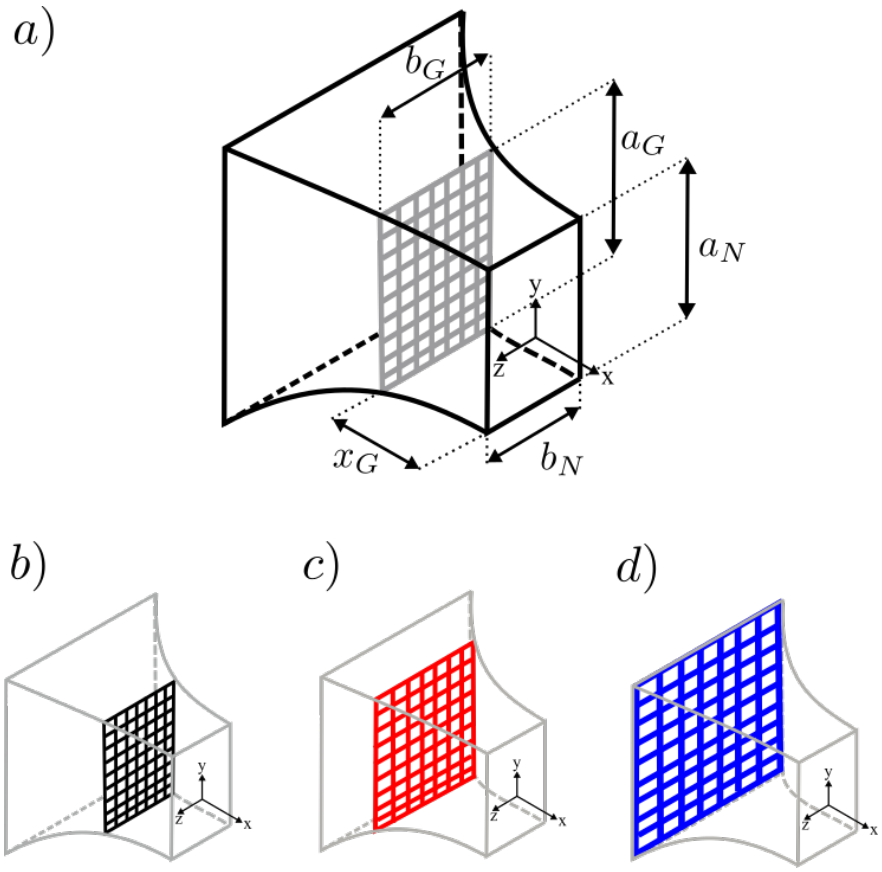

Fig. 2 Schematic of the contraction nozzle with the turbulence grids where, a) is the contraction nozzle and the defining geometry definitions, b) grid location A with a contraction ratio of 1.3, c) grid location B with a contraction ratio of 2.4, and d) grid location C with a contraction ratio of 4.4.

bar diameter. The MDF sheets were laser cut using a Trotec SP500 CO2 laser engraver for maximum accuracy of construction, an example of which is shown in Fig. 3. The size of the grids at each location are described in Table 1. The grids for both location A and location B fit in the nozzle diagonally and were held in place using polyamide thread with a high tensile strength. This was taped to each corner of the nozzle as to cause no interference to the flow. The grids at location C, the largest grids, did not fit through the nozzle in one piece and were constructed in two halves. They were joined using multiple butterfly hinges, which were fitted to the back of the grid relative to the flow to have as little influence as possible on the generation of the turbulence. Finally, a case studied was conducted to test the grids in a leading edge turbulence interaction noise set up. For this case study a NACA 0012 airfoil was used, which had a chord of 0.2 m. The airfoil was mounted in a wall bound flow with side plates that were attached to the vertical sides of the contraction nozzle. The distance between the contraction nozzle and leading edge of the airfoil was 0.65 m, this is approximately equivalent to 1 hydraulic diameter. The far field microphone array was used to measure noise emitted by the airfoil in the flow.

IV. Results and Discussion

Turbulence generation for aeroacoustic wind tunnels must not only generate a significant level of turbulence above the background intensity, but it must do so without impacting the ability to carry out direct noise measurements. This section concentrates on the far field noise for each grid that was tested and the influence of the geometric parameters on the generated noise, as well as the importance of grid location within the contraction. A case study of the interaction noise generated between the oncoming turbulence and a NACA 0012 airfoil is used as an example of the application of the grids and to assess if the grids are fit for task. The flow properties for each grid at the nozzle exit are presented first to give an indication of each grids' ability to generate turbulence.

Table 2 The geometric properties and identification of each turbulence grid and the properties of the turbulence generated by the respective grid measured at nozzle

Grid	Diameter, d (mm)	Mesh, m (mm)	σ	Turbulence intensity (%)	Integral length scale (mm)
$A-1$	6	23	0.45	4.3	10
$A-2$	6	30	0.35	4.5	11
$A-3$	10	74	0.25	8.9	17
$A-4$	16	85	0.40	12.8	18
$B-1$	10	41	0.45	4.5	13
$B-2$	10	54	0.35	4.8	14
$B-3$	17	91	0.35	7.0	17
$B-4$	25	127	0.35	8.9	19
$C-1$	19	75	0.45	4.8	12
$C-2$	19	100	0.35	4.9	13
$C-3$	32	167	0.35	8.1	17
$C-4$	45	233	0.35	10.1	19

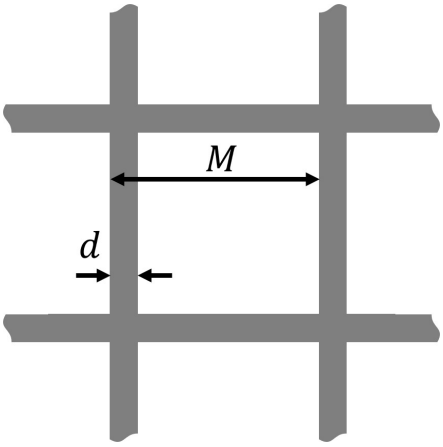

(a)

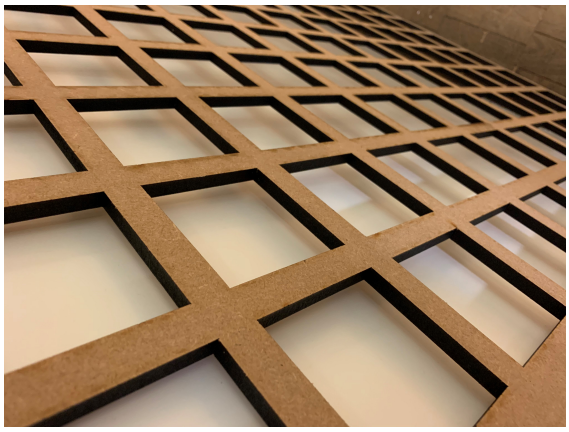

(b)

Fig. 3 Examples of the turbulence grids including, a) the defining grid dimensions and b) an example of a laser cut grid.

A. Flow properties

Table 2 displays the measured quantities for a freestream velocity of $U_\infty = 20m/s$. From the hot-wire measurements the turbulence intensity and integral length scale were calculated, where turbulence intensity is the ratio u_{rms}/U_∞. Each grid, 1-4 follows the same trend for their diameter and mesh which can be examined in Table 2. The turbulence intensity appears to follow this geometric trend for all of the grids, as the mesh size and diameter increases, the turbulence intensity increases. Grids A-1, B-1 and C-1 all generate similar levels of intensity, and with their common blockage ratio, suggests that this is an important factor in the generation of turbulence. The same is true for A-2, B-2 and C-2 although in this case they share common bar diameter to the first grid but not mesh size. This increase in mesh size leads to a small increase in turbulence intensity between A-1 and A-2, with the same being seen in grids B and C too. The highest value recorded is generated by grid A-4, with the second being grid C-4. Interestingly, the grids at location B generate similar levels of intensity for B-1 and B-2 as their counterparts at the other locations, but as the diameter and mesh size increases, grids B-3 and B-4, lower levels of turbulence intensity are generated comparatively to the corresponding grids at location A and C. This could be caused by the contraction geometry, as between location C and location B there is a large area change for a short streamwise distance. In comparison to the nozzle exit, B and C are a

similar distance from them, but there is a large geometry change for both d and M. The length scale was calculated by the curve fitting the Von Kármán Spectrum for isotropic turbulence [17], flowing the method described by Hinze [18]. To generate the curve to fit to the energy spectra the model uses the equation

$$\phi_{uu}(f) = \frac{\overline{u}'^2 \Lambda_{uu}}{\pi U_\infty} \frac{1}{(1 + (k_x/k_e)^2)^{5/6}}, \tag{2}$$

where Λ_{uu} is the integral length scale, $k_x = \omega/U_\infty$ is the stream-wise wave-number, u' is streamwise velocity fluctuation and U_∞ is the stream-wise flow velocity and

$$k_e = \frac{\sqrt{\pi}}{\Lambda_{uu}} \frac{\Gamma(5/6)}{\Gamma(1/3)}. \tag{3}$$

The value of integral length scale is changed until a good fit is achieved against the PSD of the velocity fluctuation. The results of which are displayed in Fig. 4 and are limited to one grid from each location for brevity. The full values of integral length scale for each grid are given in Table 2. These values follow a similar trend as the turbulence intensity, in that as the values of d and M increase, so does the length scale. It is also seen that the length scale generated is of the order of the size of the grid for the grids at location A, which agrees with the literature on grid generated turbulence [9]. For grids at location B and C, there is an increase in the size of the length scale, but it is not relative to the increase in d seen between the grid locations. This may be due to the increased contraction ratio straining the turbulence, but also could be due to the difficult nature of generating large scale turbulent structures. From the flow properties analysis it is evident that the grids significantly increase the level of turbulence in the flow, compared to the normal background turbulence of the wind tunnel [15]. The grids have shown that for the geometry tested it is possible to tailor the turbulence with the use of passive grids, showing effective control of the length scale and turbulence intensity of the flow. This is important in turbulence interaction studies as the level of turbulence and the size of the structures generated can affect the noise a body will generate in the flow.

B. Far field noise

This subsection displays the far field noise and highlights the difference between the individual small (A), medium (B) and large (C) grids and comparisons and differences are drawn between each set. To do so, the far field noise was recorded across the far field microphone array above the core of the jet and the Power Spectral Density of the spectrum of noise is calculated using $PSD = 10 \cdot \log_{10}(\phi_{pp}/p_{ref}^2)$ where ϕ_{pp} is the PSD of the measured acoustic pressure and $p_{ref} = 20\ \mu$Pa. The noise spectra was measured and calculated at all 23 polar angles but for brevity only the data for the 90° microphone above the core and leading edge is shown.

Figure 5 shows the normal background noise of the tunnel and noise generated by all of the small grids tested, A-1 through A-4 which have a distance from the contraction nozzle of $x_G = 500$ mm and a contraction ratio of $C = 2.4$. The first and obvious observation to make is that the self noise of all of the grids is way above the normal background noise of the jet without the grid at $U_\infty = 20$ m/s, which in some cases is in excess of 25 dB. Overall, is seems that A-1 generates most noise over the spectrum especially between 500 Hz and 4000 Hz although at frequencies less than 400 Hz all grids generate a similar level of noise. Grid A-3 generates the least noise of the smallest grids but it is still significantly louder than the background noise. Above 700 Hz although they have different levels of noise, the grids generate a similar shape over the spectrum. It is also clear that grids A-2 and A-4 generate similar levels of noise for all frequencies above 500 Hz. Referencing back to Table 2 and comparing with Fig. 5, the overall noise generated follows the same trend as the geometric property of σ, i.e. as the blockage increases, the self noise of the grid increases, as A-1 has the highest blockage ratio, and A-3 has the lowest. The self noise production, however, does not follow the same trend as the flow properties of the turbulence, and there does not seem to be a correlation between turbulence intensity or length scale and the self-noise of the grid for the smallest grids tested.

Figure 6 displays the self noise of the medium sized grids at location B, which has a distance from the contraction nozzle of $x_G = 820$ mm and a contraction ratio of $C = 2.4$, and it is evident that the position within the contraction has a profound effect on the self-noise generated by the grids. For frequencies less than 1000 Hz the noise generated by the grids could be considered to be comparative to the background noise of the tunnel at $U_\infty = 20$ m/s. However, above 1000 Hz the grids exhibit behaviour that results in tonal peaks in excess of 20 dB above the background noise. Grids B-1 and B-2 show to have the strongest humps and peaks in the spectra with B-1 being the most efficient noise generator of the four medium grids. The peaks that appear in the grids noise spectrum collapse onto a common Strouhal number when non-dimensionalized by the corresponding bar diameter, d. Grids are known to generate tonal noise [16], and due

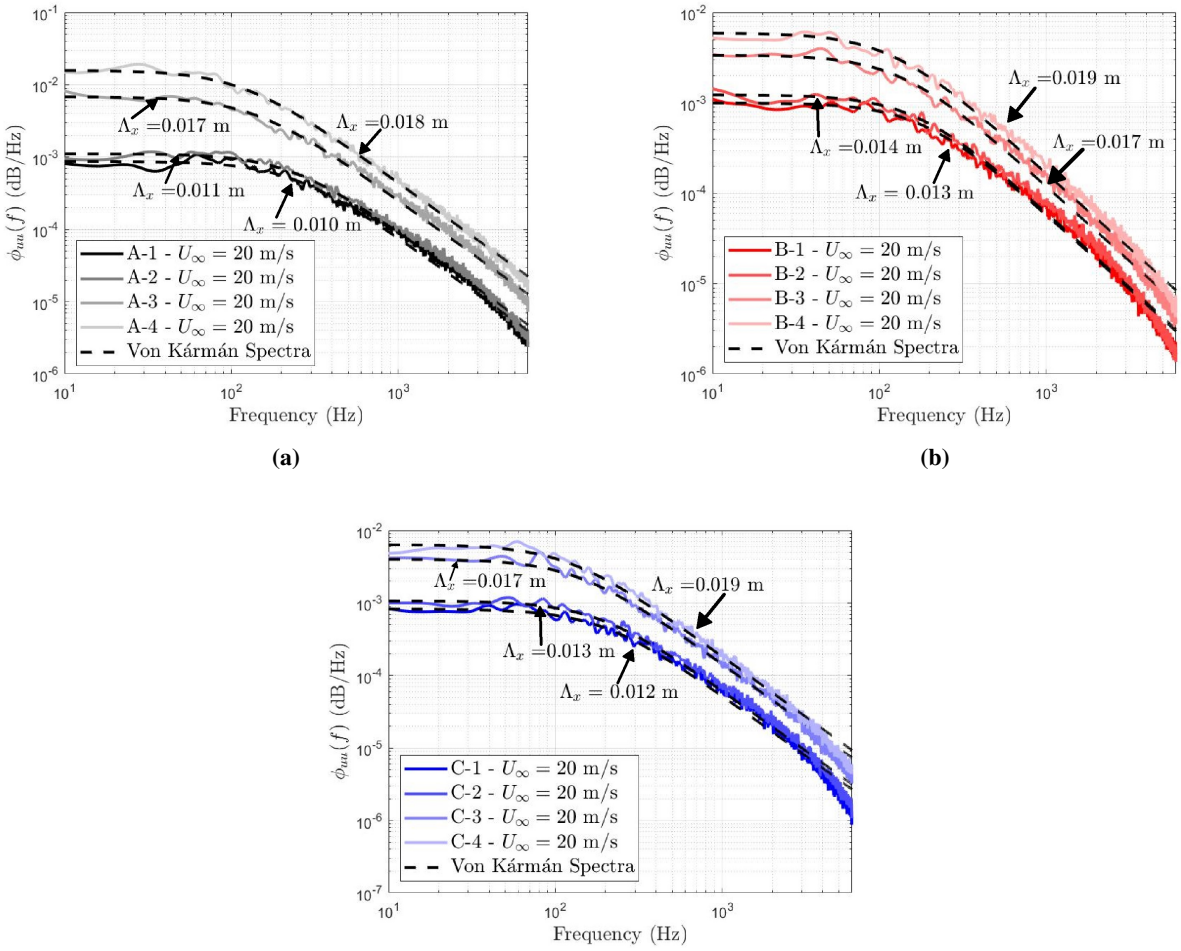

Fig. 4 Comparison of the measured stream-wise velocity spectrum ϕ_{uu} against Von Kármán model for longitudinal isotropic turbulence at $U = 20m/s$ for, (a) a small grid A-1, (b) a medium grid B-1, and (c) a large grid C-1.

to the regular geometry of the grids, the coherence between the lateral shedding is a possible source of the tones in this case. Much like the small grids, the driving factor behind the self noise appears to be the solidity factor (σ) of the grid. Grids B-2, B-3 and B-4 have a similar noise signature across the spectrum, with the exception of the peaks, and all three of these grids share the same value of σ. Grid B-4 generates the least noise of the medium grids, and apart from the tones it is within 5 dB of the background noise for the full spectrum. Referencing back to Table 2, the medium grids appear to also follow an inverse trend of the turbulence intensity and length scale, although this is not the same for the small grids. The most noise produced is by the grid that generates the lowest turbulence intensity and has the smallest length scale at the nozzle exit. Whereas the largest length scale and highest turbulence intensity generate the least self noise in B-4, with the grids B-2 and B-3 loosely following the same trend in between B-1 and B-4.

The large grids shown in Fig. 7, at location C, which has a distance from the contraction nozzle of x_G = 1040 mm and a contraction ratio of C = 4.4, offer very similar noise emission to the background of the tunnel at U_∞ = 20 m/s. For the full spectrum this is within 3 dB. All of the grid geometries show commonality across the full spectra with the background noise, although there is a similar trend to the medium grids here. Although the difference is minimal it is seen that grid C-1 generates the most noise, and grid C-4 appears to generate the least. Again, referencing Table 2, this is an inverse trend to the turbulence properties but it does have commonality with the effect of changing σ. As the grids show little effect on the background noise that is generated when comparing with the turbulent flow properties they

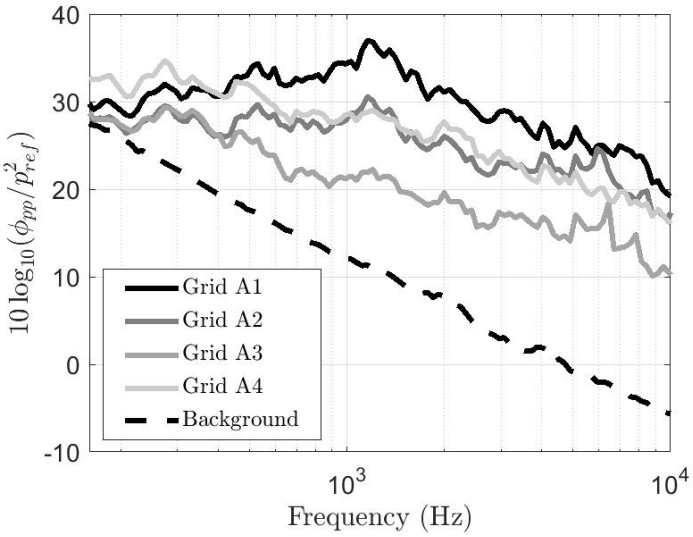

Fig. 5 Comparison of the far field noise produced by each small grid at location A with a contraction ratio of $C = 1.3$, and the background noise with no grid at $U_\infty = 20$ m/s.

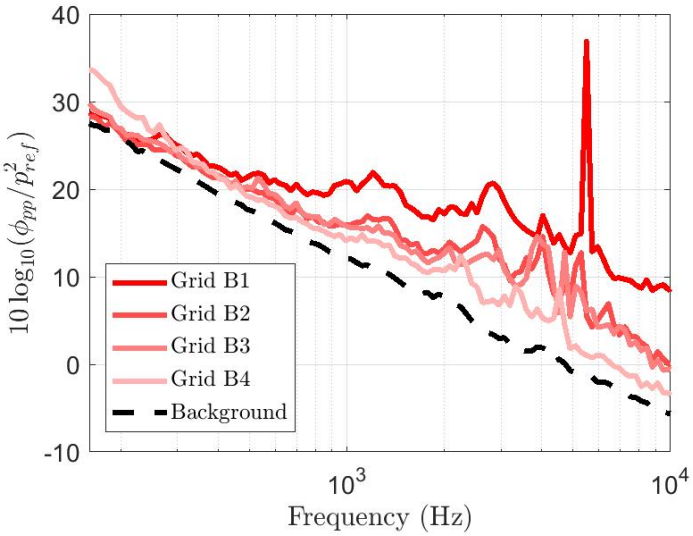

Fig. 6 Comparison of the far field noise produced by each medium grid at location B with a contraction ratio of $C = 2.4$, and the background noise with no grid at $U_\infty = 20$ m/s.

produce, it is hard to suggest if this has an effect on the self noise that grids generate for the location A grids and location B grids. Because the turbulence generated by the location C grids will have very little effect on the typical background noise generated by a smooth flow, this makes them an ideal candidate for turbulence interaction noise studies. From Figs. 5, 6 and 7 it is clear that the main factor in the generation of the noise by turbulence grids is the impingement velocity on the grid, and geometrically the openness ratio has next most significant effect.

Figure 8 is the example of the noise spectra in the case study, and shows the normal tunnel background noise, background noise of the grid and then the interaction noise between the NACA 0012, of chord 0.2 m and positioned 0.65 m from the contraction nozzle exit, and the turbulent flow. The first from each of the locations was chosen as these generate the most background noise, and from the figure it can be seen that the self-noise of the grid has a profound effect on the interaction noise, and in the case of grids A-1 and B-1, it is not separable from the interaction noise.

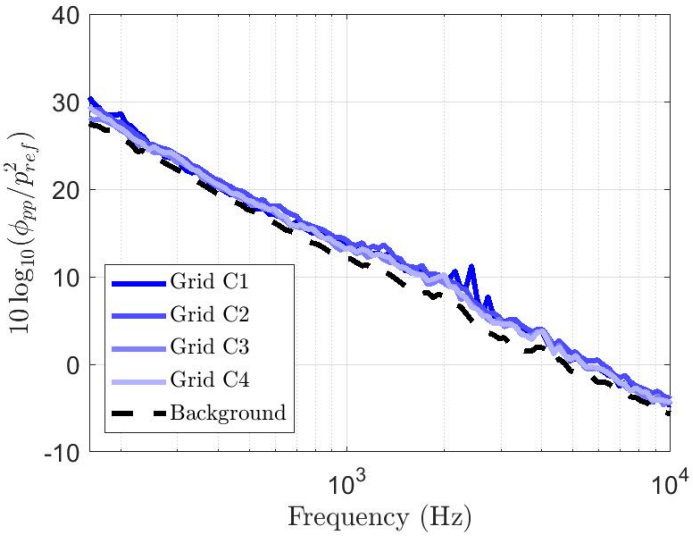

Fig. 7 Comparison of the far field noise produced by each large grid at location C with a contraction ratio of $C = 4.4$, and the background noise with no grid at $U_\infty = 20$ m/s.

A-1 shows a very similar noise spectrum between the grid noise and the interaction noise. Whereas there is some distinguishable differences between interaction noise and the grid noise for B-2, above 1000 Hz the self-noise of the grid affects the interaction noise. For grid C-1, there is a clear difference between the interaction noise and the background noise of the grid across the full spectrum, less than 1000 Hz the interaction noise is dominant. Above 1000 Hz there is still a difference, but due to turbulence interaction noise being a low frequency phenomena the difference is expected to be at lower frequencies. To illustrate the difference between the interaction noise and self noise of all the grids tested the ΔPSD was calculated as $\Delta PSD = PSD_{NACA} - PSD_{grid}$ which is displayed in Fig. 9. This figure shows a clearer picture of how the geometric effects of the grid generate different turbulent flow properties, which in turn affects the noise generated in the interaction between the flow and the airfoil leading edge. Figure 9 shows how the grid geometry affects the interaction noise and shows an increase in Δ PSD from location A through to location C. This supports the suggestion that the grids' location within the contraction (x_G) and subsequent contraction ratio (C) are the key parameters for grid design in the context of aeroacoustic applications. Grids at location A, $C = 1.3$, show the lowest difference between the interaction noise and the grid noise, and from 160 Hz, it decays to a near-zero difference above 1000 Hz. The grids at location B, $C = 2.4$, show an improvement over the location A grids in terms of the ΔPSD, but at higher frequencies above 1000 Hz, the aeolian tones that the grids produce contaminate the noise signature. The large grids, at location C $C = 4.4$, show the largest difference between the interaction noise and the grid noise, and even above 1000 Hz there is still a difference seen, although the dominant noise source is the interaction noise at lower frequencies. When considering the figure as a whole, a comparison between the turbulence properties and the generated interaction noise can be deduced. The grids that generate the largest length scale and highest turbulence intensity seem to generate the most interaction noise with the NACA 0012 above the background noise. In all cases, the grids with the lowest d and M values generate the least interaction noise, and the largest values generate the most. The grids with geometric values in between this also fit the trend. As these geometric properties dictate the turbulence properties that are generated, it can be suggested that the geometry in this case dictates the interaction noise generated. It is difficult to suggest whether this is an effect of the turbulence intensity, or the length scale, or a combination of the both, as there is no case with a decreasing length scale and increased turbulence intensity, or vice versa. From this, the largest grids at location C appear to be the best candidate for direction measurement of turbulence interaction, as they have the least affect on the background noise but are still capable of generating similar turbulence properties to smallest grids and the nozzle exit. However, the small and medium grids are still suitable for aeroacoustic turbulence studies although direct measurement is not recommended, and instead a more suitable method for the study of far field noise would be a microphone array beamforming technique.

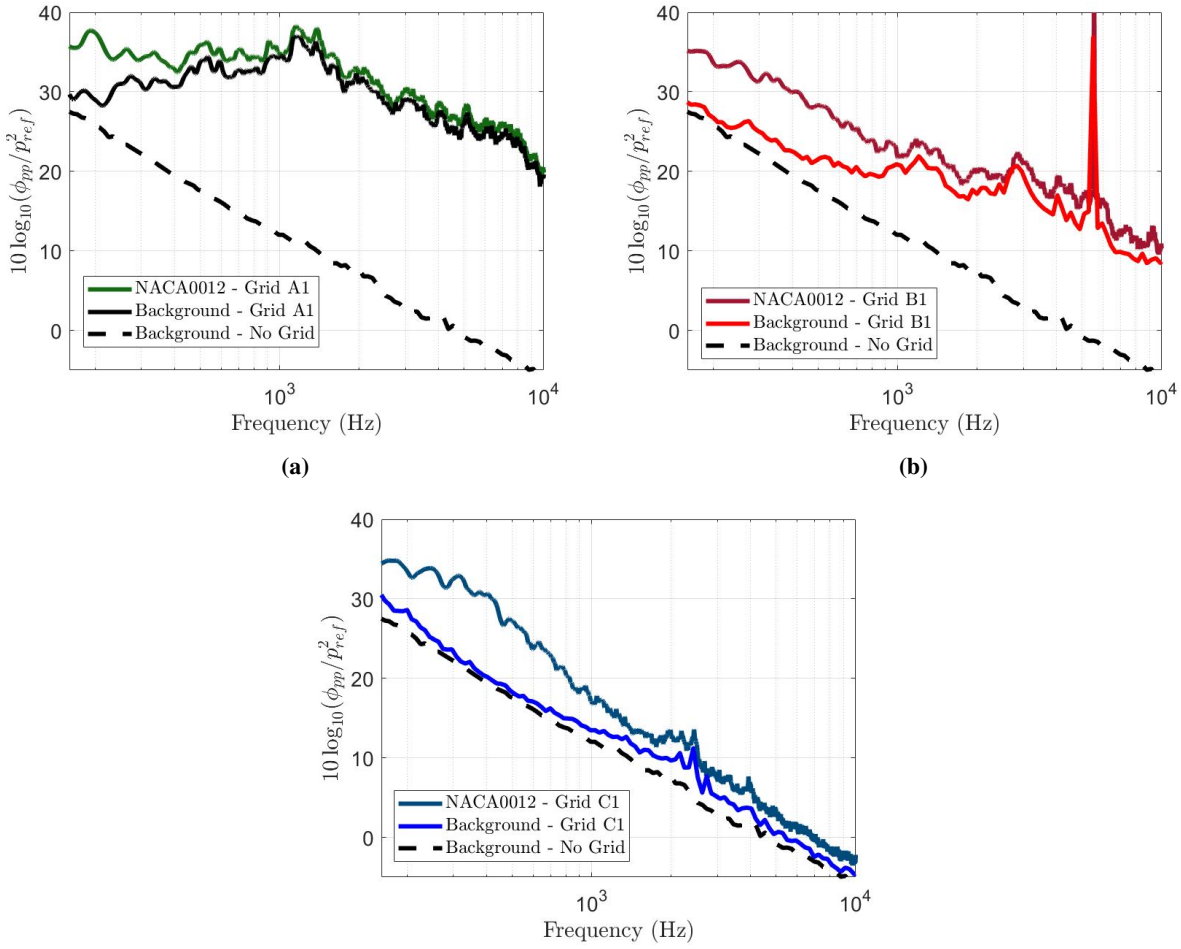

Fig. 8 Power spectral density of the turbulence interaction noise generated by a NACA 0012 airfoil at $\alpha = 0°$, the background noise of the grid, and the normal background noise of the tunnel without a grid for, a) grid A1 where $C = 1.3$, b) grid B1 where $C = 2.4$, c) grid C1 where $C = 4.4$.

V. Conclusion

The flow properties highlighted that it is possible to control the generation of turbulence using passive grids. Changes in the geometry, d and M, show that they affect the generated turbulence intensity and length scale. As the grids get larger and are positioned further into the contraction, the geometry is scaled to match the area increase, although this increasing geometry does not increase the flow structures in the same ratio. In terms of the noise that is generated by the grids, the most important geometric quantity is shown to the the ratio of the nozzle exit and the grid size. The larger this ratio is the less self noise they will generate, and provided the geometry is scaled with the area change, then similar levels of turbulence intensity and size of length scale is achievable. The largest grids tested showed that it is possible to carry out direct noise measurement and generate a comparable level of turbulence to the smallest grids. Ideally, for direct measurement of far field noise, it would be suggested to have a grid far inside the contraction that is still capable of generating a high enough level of turbulence. However, it would be important to note that the isotropy of the flow, and how the flow develops downstream requires further study.

Acknowledgments

The authors would like to acknowledge the financial support of Embraer S.A. and EPSRC.

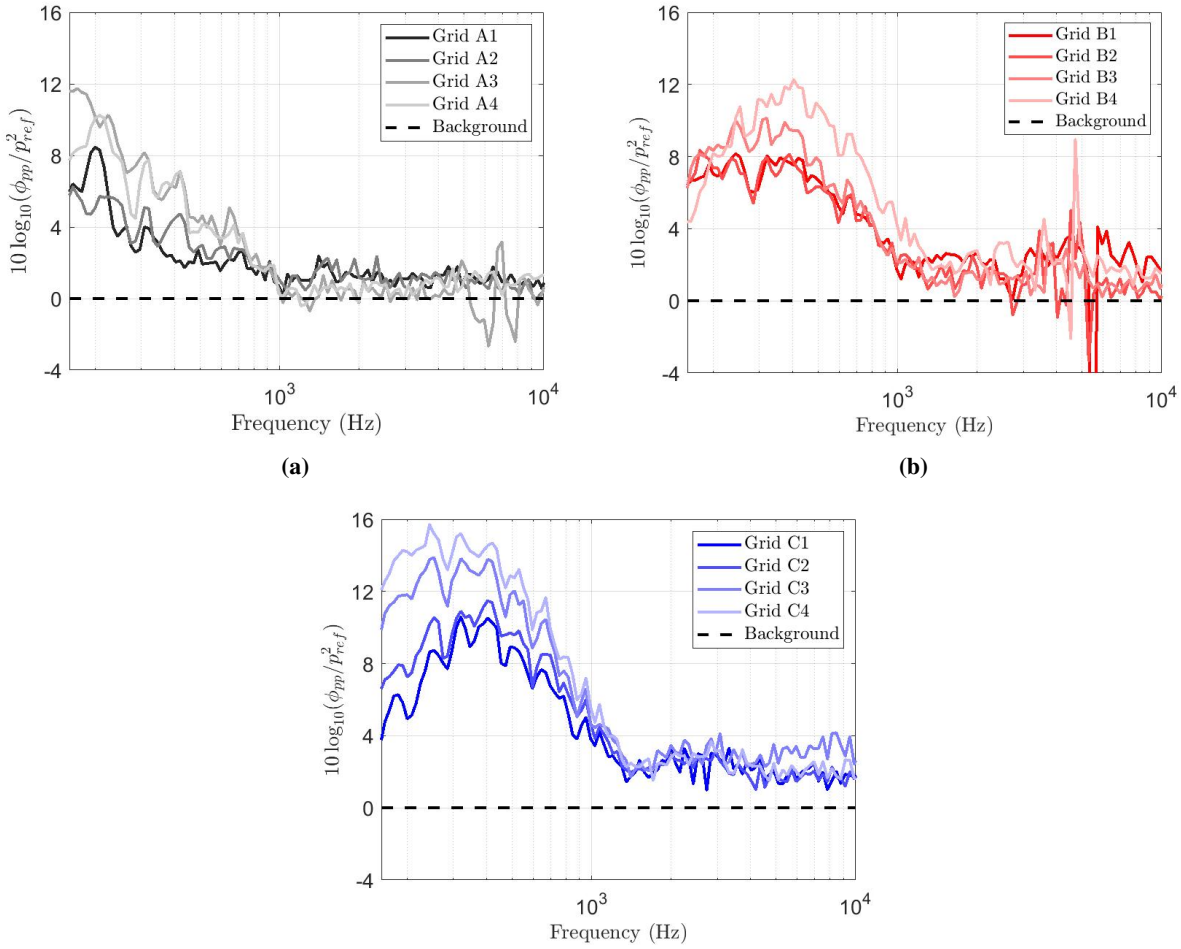

Fig. 9 Δ PSD between the background noise of the grid, and the turbulence interaction noise generated by a NACA 0012 airfoil at $\alpha = 0°$ for a) Location A where $C = 1.3$, b) Location B where $C = 2.4$ and c) Location C where $C = 4.4$..

References

[1] Lyu, B., and Azarpeyvand, M., "On the noise prediction for serrated leading edges," *Journal of Fluid Mechanics*, Vol. 826, 2017, p. 205–234. https://doi.org/10.1017/jfm.2017.429.

[2] Kim, J., Haeri, S., and Joseph, P., "On the reduction of aerofoil-turbulence interaction noise associated with wavy leading edges," *Journal of Fluid Mechanics*, Vol. 792, 2016, pp. 526–552. Data files are made available from http://dx.doi.org/10.5258/SOTON/397245 as required by EPSRC Research Data Policy.

[3] Narayanan, S., Chaitanya, P., Haeri, S., Joseph, P., Kim, J. W., and Polacsek, C., "Airfoil noise reductions through leading edge serrations," *Physics of Fluids*, Vol. 27, No. 2, 2015, p. 025109. https://doi.org/10.1063/1.4907798.

[4] Chaitanya, P., Joseph, P., Narayanan, S., Vanderwel, C., Turner, J., Kim, J. W., and Ganapathisubramani, B., "Performance and mechanism of sinusoidal leading edge serrations for the reduction of turbulenceaerofoil interaction noise," *Journal of Fluid Mechanics*, Vol. 818, 2017, pp. 435–464. https://doi.org/10.1017/jfm.2017.141.

[5] Roger, M., Schram, C., and Santana, L. D., *Reduction of Airfoil Turbulence-Impingement Noise by Means of Leading-Edge Serrations and/or Porous Material*, chapter and pages. https://doi.org/10.2514/6.2013-2108.

[6] Geyer, T. F., Lucius, A., Schrödter, M., Schneider, M., and Sarradj, E., "Reduction of Turbulence Interaction Noise

Through Airfoils With Perforated Leading Edges," *Acta Acustica united with Acustica*, Vol. 105, No. 1, 2019, pp. 109–122. https://doi.org/doi:10.3813/AAA.919292.

[7] Geyer, T., Sarradj, E., Giesler, J., and Hobracht, M., *Experimental assessment of the noise generated at the leading edge of porous airfoils using microphone array techniques*, chapter and pages. https://doi.org/10.2514/6.2011-2713.

[8] Simmons, L. F. G., Salter, C., and Taylor, G. I., "Experimental investigation and analysis of the velocity variations in turbulent flow," *Proceedings of the Royal Society of London. Series A, Containing Papers of a Mathematical and Physical Character*, Vol. 145, No. 854, 1934, pp. 212–234. https://doi.org/10.1098/rspa.1934.0091.

[9] Roach, P., "The generation of nearly isotropic turbulence by means of grids," *International Journal of Heat and Fluid Flow*, Vol. 8, No. 2, 1987, pp. 82 – 92. https://doi.org/https://doi.org/10.1016/0142-727X(87)90001-4.

[10] Lavoie, P., Burattini, P., Djenidi, L., and Antonia, R. A., "Effect of initial conditions on decaying grid turbulence at low Rλ," *Experiments in Fluids*, Vol. 39, No. 5, 2005, pp. 865–874. https://doi.org/10.1007/s00348-005-0022-8.

[11] Uberoi, M. S., and Wallis, S., "Effect of Grid Geometry on Turbulence Decay," *The Physics of Fluids*, Vol. 10, No. 6, 1967, pp. 1216–1224. https://doi.org/10.1063/1.1762265.

[12] Comte-Bellot, G., and Corrsin, S., "The use of a contraction to improve the isotropy of grid-generated turbulence," *Journal of Fluid Mechanics*, Vol. 25, No. 4, 1966, pp. 657–682. https://doi.org/10.1017/s0022112066000338.

[13] Batchelor, G. K., Townsend, A. A., and Taylor, G. I., "Decay of vorticity in isotropic turbulence," *Proceedings of the Royal Society of London. Series A. Mathematical and Physical Sciences*, Vol. 190, No. 1023, 1947, pp. 534–550. https://doi.org/10.1098/rspa.1947.0095.

[14] Paruchuri, C., Gill, J. R., Subramanian, N., Joseph, P., Vanderwel, C., Zhang, X., and Ganapathisubramani, B., *Aerofoil geometry effects on turbulence interaction noise*, chapter and pages. https://doi.org/10.2514/6.2015-2830.

[15] Mayer, Y. D., Jawahar, H. K., Szőke, M., Ali, S. A. S., and Azarpeyvand, M., "Design and performance of an aeroacoustic wind tunnel facility at the University of Bristol," *Applied Acoustics*, Vol. 155, 2019, pp. 358 – 370. https://doi.org/https://doi.org/10.1016/j.apacoust.2019.06.005.

[16] Devenport, W. J., Staubs, J. K., and Glegg, S. A., "Sound radiation from real airfoils in turbulence," *Journal of Sound and Vibration*, Vol. 329, No. 17, 2010, pp. 3470 – 3483. https://doi.org/https://doi.org/10.1016/j.jsv.2010.02.022.

[17] von Kármán, T., "Progress in the Statistical Theory of Turbulence," *Proceedings of the National Academy of Sciences*, Vol. 34, No. 11, 1948, pp. 530–539. https://doi.org/10.1073/pnas.34.11.530.

[18] Hinze, J., *Turbulence:*, McGraw-Hill classic textbook reissue series, McGraw-Hill, 1975.